873. Cogging torque and torque ripple reduction of a novel exterior-rotor geared motor

Yi-Chang Wu[1], Yi-Cheng Hong[2]
National Yunlin University of Science & Technology, Yunlin, Taiwan, R. O. C.
E-mail: [1]*wuyc@yuntech.edu.tw*, [2]*g9911765@yuntech.edu.tw*

(Received 28 June 2012; accepted 4 September 2012)

Abstract. The reduction of cogging torque and torque ripple in permanent-magnet motors to suppress the vibration and acoustic noise is a major concern for motor designers. This study presents a novel exterior-rotor geared motor which integrates a brushless permanent-magnet (BLPM) motor with an epicyclic-type gear reducer to form a compact structural assembly without extra transmitting elements. One of the special features of the geared motor lies in the gear-teeth of the epicyclic-type gear reducer merged with the stator of the BLPM motor. The gear-teeth serve as the interfacial medium to connect the BLPM motor with the epicyclic-type gear reducer, which provides functions not only for transmission to achieve a desired speed ratio, but also effectively reduce the cogging torque and torque ripple of the geared motor. Five shape models of pole shoes with different values of the shoe depth and the shoe ramp are presented to effectively reduce the cogging torque and the torque ripple. With the aid of the finite-element analysis, shape model III of the geared motor performs better than the existing BLPM motor on the cogging torque with 87 % decreasing and the torque ripple with 23 % decreasing. Such a unique characteristic of the geared motor is of benefit to the widely applications on accurate motion and position control systems.

Keywords: cogging torque reduction, torque ripple reduction, geared motor, brushless permanent-magnet motor, epicyclic-type gear reducer.

Introduction

A geared motor, which comprises an electric motor and a gear reducer, is an electromechanical device to adjust rotational speed and output torque to meet needed drive requirements. It has found more and more applications in high driving torque, low rotational speed, and high-precision speed and position control applications, such as industrial robots, machine tools, automatic conveying equipments, and office automation apparatuses. As for electric motors, the brushless permanent-magnet (BLPM) motor has the characteristics of high efficiency, light weight, high torque-to-volume ratio, and easy speed control, which is widely used to be the power source of the geared motor. However, there are two fluctuated torque components in the output torque of the BLPM motor that affect the control accuracy and cause undesirable vibration, noise, and mechanical resonance. One is the cogging torque, which arises from the interaction of permanent magnets on the rotor and the slotted structure of the stator. The other is the ripple torque, which is generated by the interaction of the harmonics of armature currents with those of the induced back electromotive forces. The sum of the cogging and ripple torque components is the pulsating torque or torque ripple [1]. Since the torque ripple prevents a smooth rotation of the BLPM motor, it is a major concern for motor designers and should be minimized to avoid vibration and position inaccuracy. Generally speaking, feasible techniques for pulsating torque minimization can be classified into two major categories, i.e., the motor design techniques and the control techniques. However, the most effective and straightforward means to minimize the torque ripple is by proper motor design [1]. Numerous methods have been developed to attempt minimizing the cogging torque and pulsating torque of permanent-magnet motors. Skewing of the stator lamination or the rotor magnetization is the most common approach for this purpose, which reduces the harmonic content in the slots by uniformly distributing the magnetic field [2]. The stepped skewing of permanent-magnet blocks

[1], which cancel all cogging torque harmonics except for the multiples of the number of the blocks, can be used if the rotor skewing is not practical. Placing auxiliary salient poles on the stator [3, 4], dummy slots on the pole face of the armature core [5, 6], and auxiliary slots on the magnetizing yoke of permanent magnets [7], are effective methods for pulsating torque minimization due to the design strategy to increase the torque frequency and hence decrease its amplitude. Furthermore, other motor design techniques, including: configuration designs with fractional slot-to-pole ratios [8], geometry designs by providing teeth pairings with two different types of tooth width [9], modifying permanent magnet arc [10, 11], optimizing saliency and teeth shape [12, 13], adjusting slot openings [14], and shifting the pole pairs by half a slot pitch [15], are all available means for reducing the cogging torque as well as the torque ripple. Although these methods are effective for reducing the cogging torque and torque ripple of BLPM motors, they may result in complex structure and increase the manufacturing cost and maintenance complexity especially for geared motors. In order to reduce the mechanical components as well as the pulsating torque of the geared motor, it is possible to integrate the gear element with the motor element to form a single mechanical part from the structural point of view. Fewer mechanical components decrease production costs, improve the reliability, and make the whole device more compact, lightweight, and easier for maintenance. Besides, the integrated mechanical parts may alter the geometric configurations of the rotor or stator and affect the magnetostatic field, which offers the opportunities to reduce the cogging torque and torque ripple of the BLPM motor.

This study proposes a novel geared motor which integrates an exterior-rotor BLPM motor with an epicyclic-type gear reducer without extra transmitting elements. In what follows, the configuration and features of the geared motor are presented. A commercially available finite-element package Ansoft/Maxwell is used to calculate the cogging torque and electromagnetic torque of the geared motor. The cogging torque and torque ripple of the geared motor are discussed and compared with an existing BLPM motor that has similar motor dimensions and identical magnet material properties.

A novel exterior-rotor geared motor

The BLPM motor is essentially configured as alternate magnet poles rotating past stationary conductors that carry the current. For a BLPM motor with an exterior-rotor configuration, the rotor appears on the outside of the stator. The main features of the exterior-rotor BLPM motor are simple to wind and easy to manufacture, which results in low product cost. In addition, the relative large rotor diameter increases the moment inertia, which in turn helps to maintain constant rotational speed. Based on a 3-phase, 12-pole/18-slot exterior-rotor BLPM motor and a 5-link, 2-degrees-of-freedom (2-DOF) epicyclic-type gear train, a novel geared motor with an exterior-rotor configuration is proposed. Fig. 1(a) and Fig. 1(b) respectively show the cutaway view and exploded view of the proposed geared motor. As can be seen in Fig. 1(b), member 0 is the frame of the geared motor. Member 1 is the sun gear which is affixed to the stator of the motor to be the fixed link of the epicyclic-type gear train. Member 2 is the carrier integrated with the output casing. It is also the output link of the epicyclic-type gear train. Member 3 is the ring gear of the epicyclic-type gear train connected with the exterior-rotor of the motor to form a single structural assembly. So, the ring gear is the input link of the epicyclic-type gear train. Member 4 is the planet gear. Two identical planet gears are used to engage with the ring gear and the sun gear for increasing load capacity and providing better balancing of gear tooth load and inertia force. Member 5 is the permanent magnet affixed to the inner yoke surface of member 3 to prevent the magnet from flying apart especially in high-speed applications. Member 6 is the stator which comprises of a lamination of magnetic steel slices to reduce the eddy current losses. Member 7 is the phase winding. The frame (member 0) and the output casing (member 2) of the geared motor use ventilation holes to easily dissipate the heat from the

stator. Unlike existing geared motors in the current market that connect casings of gear reducers with stators of electric motors by connectors and mechanical fasteners, a special feature of the proposed design is the external gear-teeth of the sun gear merged with the pole shoes of the stator, as shown in Fig. 2. The addendum circle of the sun gear is coincident with the outer edge of the stator. Each slot opening of the stator is formed by removing the bottom land of the sun gear. It enables the copper conductors to set into the slot areas, and also does not affect the conjugate relation for gear meshing. Since the exterior gear-teeth are integrated on the stator, the punching process forms the slices of the sun gear and the stator simultaneously with the same punching die to reduce the manufacturing cost. Moreover, unlike the traditional manufacturing process of cut gears, the sun gear is made up of stacking identical laminations of punched steel slices. The 5-link epicyclic-type gear train shown in Fig. 1 is the simplest epicyclic-type gear train in the planetary gear train family, and the related kinematic equation is:

$$\gamma_{43}\omega_1 + (\gamma_{41} - \gamma_{43})\omega_2 - \gamma_{41}\omega_3 = 0, \quad (1)$$

where gear ratios $\gamma_{41} = -Z_4 / Z_1$, $\gamma_{43} = Z_4 / Z_3$, and Z_i is the number of teeth on gear i. In this geared motor, the teeth numbers Z_1, Z_3 and Z_4 are 126, 182 and 28, respectively. It is noted that the number of teeth of the sun gear is a multiple of the number of stator slots due to the gear-teeth of the sun gear placed at regular intervals on the stator. Because the sun gear is the fixed link, we have $\omega_1 = 0$. The speed ratio, which is defined as the ratio of the input link speed to the output link speed, of the epicyclic-type gear train shown in Fig. 1 is $\omega_3 / \omega_2 = (Z_1+Z_3)/Z_3 = (126+182)/182 = 1.69$. Since the speed ratio of the epicyclic-type gear train is greater than one, it is a gear reducer that provides the function of speed reduction.

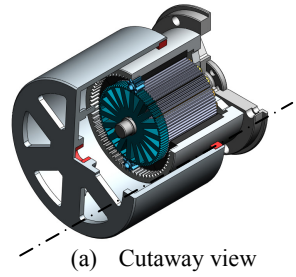

(a) Cutaway view

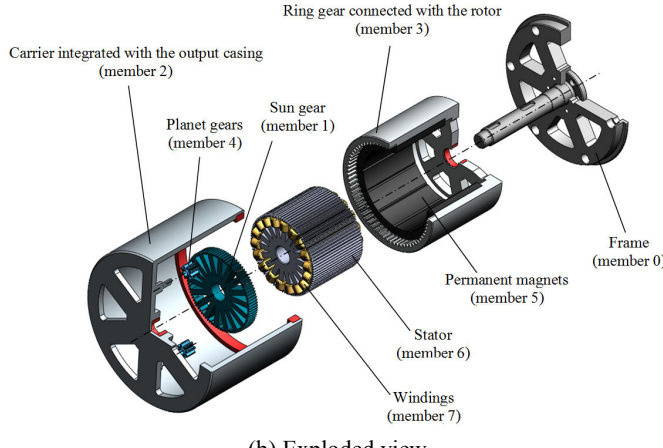

(b) Exploded view

Fig. 1. The proposed geared motor with an exterior-rotor configuration

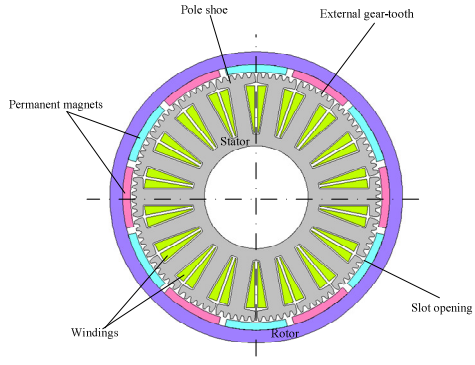

Fig. 2. Cross section of the geared motor shown in Fig. 1

Cogging torque and torque ripple reduction

The BLPM motor exhibits an inherent cogging torque that causes vibration as well as prevents a smooth rotation. Such a pulsating torque is detrimental to the motor performance, especially in high-precision speed and position control applications. As mentioned earlier, the cogging torque of the permanent-magnet motor arises from the mutual interaction of permanent magnets and the stator slotted structure as the rotor rotates relative to the stator. Since the cogging torque is greatly affected by the configuration of the stator, the prediction of the cogging torque for the proposed geared motor with external gear-teeth integrated on the stator is an essential task, and its reduction becomes one of the major goals of this study. In [16], the n-th harmonic components that cause the cogging torque are:

$$n = i\frac{T}{\gcd(P,\ T)},\ i = 1,\ 2,\ 3,\ ... \tag{2}$$

where $\gcd(P,\ T)$ is the greatest common divisor between P and T, P is the number of magnet poles, and T is the number of slot-teeth or the gear-teeth integrated on the stator. It implies that the orders of the harmonic components that dominate the cogging torque are directly related to the number of gear-teeth on the stator and the number of magnet poles on the rotor. For the geared motor shown in Fig. 2, it is designed with 12 magnet poles on the rotor and 126 external gear-teeth integrated on the stator. The n-th harmonic components that generate the cogging torque of the existing BLPM motor and the geared motor are respectively shown in Table 1. For the existing 12-pole/18-slot BLPM motor, the number of stator teeth is equal to 18, and the dominant harmonic components of the cogging torque are of order $3i$ (i = 1, 2, 3, …). For the proposed geared motor with 126 gear-teeth placed at regular intervals on the stator, the harmonic components that generate the cogging torque turn into order $21i$. This means that the first twenty harmonic components of the cogging torque vanish theoretically. Both of these two motors are with fractional tooth-to-pole ratios. Mathematically, the magnitude of the harmonic component usually decreases in accordance with the increase of its order number. The strategy for reducing the cogging torque is to make the dominant harmonic components with higher order numbers through properly determining the numbers of gear-teeth on the stator and magnet poles on the rotor. In order to verify the correctness and effectiveness of the above analysis, finite element calculation by using the commercial finite-element package Ansoft/Maxwell is carried out to compute the cogging torque. The neodymium-iron-boron (NdFeB) magnet is employed to the existing BLPM motor and the geared motor for excitation. In order to make a quantitative comparison, the main geometric dimensions and magnet material properties of the geared motor are set to be identical with those of an existing BLPM motor, as shown in Table 2.

The cross-section and geometric parameters of the geared motor are presented in Fig. 3. Fig. 4 illustrates the distributions of cogging torques for these two motors by using Ansoft/Maxwell. The period of the stable equilibrium position of the cogging torque for the permanent-magnet motor is [17]:

$$\theta_s = \frac{360^\circ}{\text{lcm}(P,T)}, \tag{3}$$

where θ_S is the period of the stable equilibrium position in mechanical degree and lcm(P, T) is the least common multiplier between P and T. As can be seen in Table 1 and Fig. 4, the periods of the stable equilibrium position of the cogging torque for the existing BLPM motor and the proposed geared motor are 10° and 1.43°, respectively. We can find the geared motor increases the frequency of the cogging torque, and hence decreases its amplitude. According to Fig. 4, the peak values of cogging torques for the existing BLPM motor and the geared motor are 2.85 Nm and 0.35 Nm, respectively. The geared motor performs better than the existing BLPM motor on the cogging torque with 87.7 % decreasing. Therefore, the geared motor with gear-teeth on the stator effectively eliminates the cogging torque.

Table 1. Harmonic components that generate the cogging torque of the existing motor and proposed motor

Case	P	T	T/P	gcd(P, T)	n	lcm(P, T)	θ_s
Existing BLPM motor	12	18	1.5	6	$3i$	36	10°
Proposed geared motor	12	126	10.5	6	$21i$	252	1.43°

Table 2. Corresponding values of magnet properties and main dimensions of the geared motor

Magnet properties (NdFeB)		
Items	Symbol	Values
Remanence (T)	B_r	0.76
Coercivity (A/m)	H_c	-480000
Relative permeability	μ_r	1.26
Direction of magnetization	--	radial
Magnet thickness (mm)	l_m	6
Magnet arc (degree)	θ_m	27
Motor parameters		
Items	Symbol	Values
Number of phases	N_{ph}	3
Number of magnet poles	P	12
Number of magnet slots	S	18
Number of gears	T	126
Module	m	1.5
Air gap length (mm)	g	1
Slot opening width of stator (mm)	w_s	1.2
Outer radius of rotor (mm)	R_{ro}	113
Inner radius of rotor (mm)	R_{ri}	97
Outer radius of stator (mm)	R_{so}	100
Inner radius of stator (mm)	R_{si}	40
Tooth width of stator (mm)	W_{tb}	12
Shoe depth (mm)	d_1	4
Shoe ramp (degree)	d_2	0
Number of coils per armature tooth (turn)	N_c	54
Stack length (mm)	L	25
Rated phase current (A)	i_{ph}	10

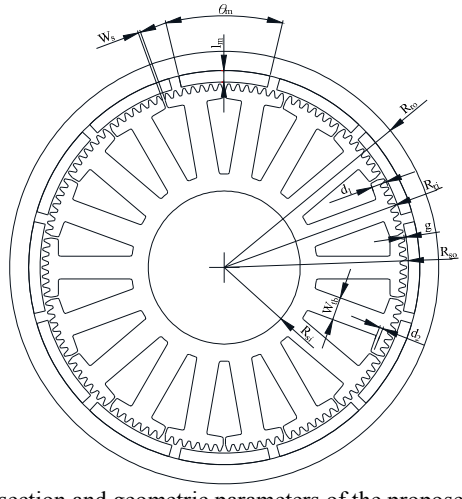

Fig. 3. Cross-section and geometric parameters of the proposed geared motor

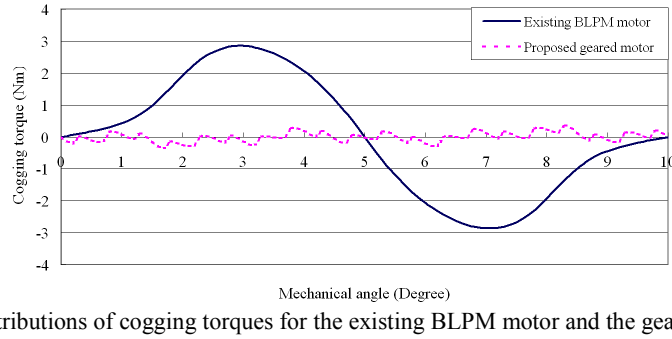

Fig. 4. Distributions of cogging torques for the existing BLPM motor and the geared motor

For the above two motors, each phase current is operated with square wave excitation as shown in Fig. 5. Two phases are conducting simultaneously at each time and the rated current value is equal to 10A. The winding layout of the 3-phase geared motor is listed in Fig. 6(a), while the winding configuration is schematically shown in Fig. 6(b). The electromagnetic torques of the existing BLPM motor and the geared motor are illustrated in Fig. 7. The torque ripple is the difference between the minimum and maximum electromagnetic torque divided by the average electromagnetic torque. As can be seen in Table 3, the geared motor performs better than the existing BLPM motor on the torque ripple with 9.9 % decreasing.

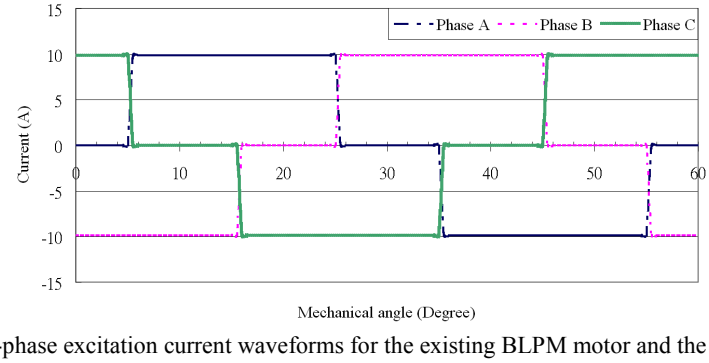

Fig. 5. Three-phase excitation current waveforms for the existing BLPM motor and the geared motor

Slot	Phase A	Phase B	Phase C
1	In		Out
2	Out	In	
3		Out	In
4	In		Out
5	Out	In	
6		Out	In
7	In		Out
8	Out	In	
9		Out	In
10	In		Out
11	Out	In	
12		Out	In
13	In		Out
14	Out	In	
15		Out	In
16	In		Out
17	Out	In	
18		Out	In

(a) winding layout

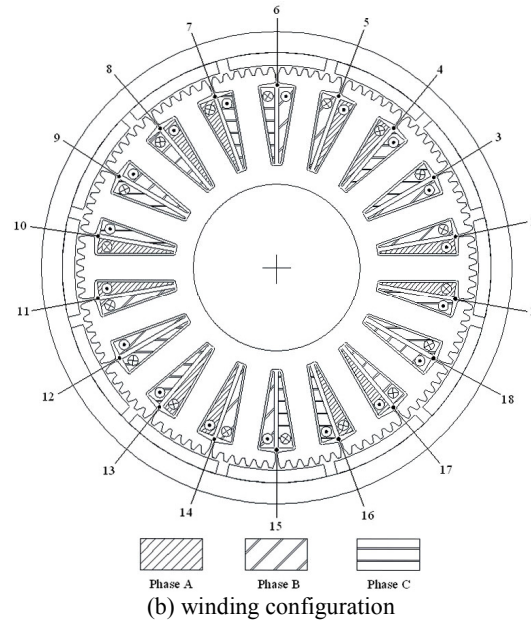

(b) winding configuration

Fig. 6. Winding layout and winding configuration of the proposed 3-phase geared motor

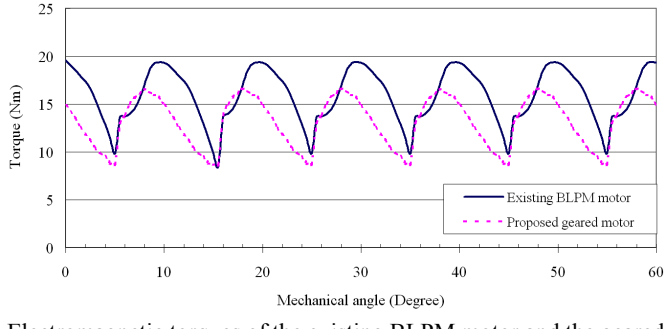

Fig. 7. Electromagnetic torques of the existing BLPM motor and the geared motor

Table 3. Torque ripples of the existing BLPM motor and the geared motor

Case	Max. value (Nm)	Min. value (Nm)	Average value (Nm)	Torque ripple (%)
Existing BLPM motor	19.60	8.48	15.81	70.3
Proposed geared motor	16.60	8.65	13.17	60.4

Shape design of pole shoes

For the study of cogging torque and torque ripple related to the shape design of pole shoes, five shape models with different values of the shoe depth d_1 and the shoe ramp d_2 are presented as shown in Table 4 and Fig. 8. Shape model I is the case shown in Table 2. The commercial finite-element package Ansoft/Maxwell is also employed to calculate the cogging torque and electromagnetic torque of these five models. Fig. 9 presents the cogging torque waveform according to the shape models. From the analysis results, we can find that these five models possess similar cogging torques. Fig. 10 shows the electromagnetic torque of each shape model. As illustrated in Table 4, shape model III has the largest average electromagnetic torque and the

smallest torque ripple among them. Shape model III performs better than the existing BLPM motor on the torque ripple with 23.8 % decreasing.

Table 4. Electromagnetic torques and torque ripples of five shape models

Model	Parameters	Max. value (Nm)	Min. value (Nm)	Average value (Nm)	Torque ripple (%)
I	$d_1 = 4$ mm, $d_2 = 0°$	16.60	8.65	13.17	60.4
II	$d_1 = 5$ mm, $d_2 = 15°$	16.58	9.02	13.61	55.6
III	$d_1 = 6$ mm, $d_2 = 0°$	16.60	10.10	13.99	46.5
IV	$d_1 = 6$ mm, $d_2 = 15°$	16.21	8.90	13.25	55.2
V	$d_1 = 7$ mm, $d_2 = 0°$	16.56	9.26	13.56	53.8

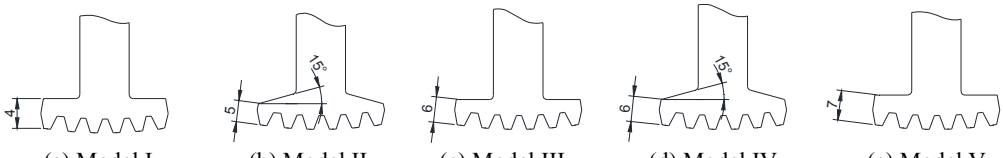

(a) Model I (b) Model II (c) Model III (d) Model IV (e) Model V

Fig. 8. Five shape models with different values of the shoe depth and the shoe ramp

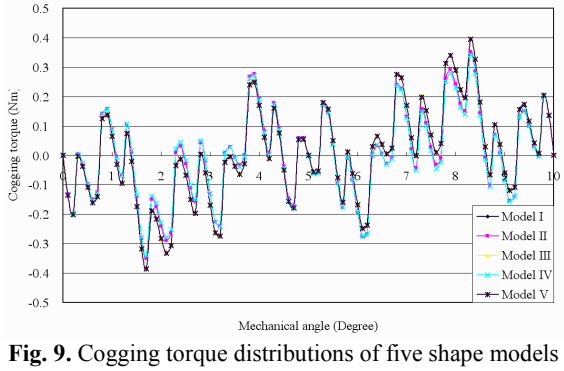

Fig. 9. Cogging torque distributions of five shape models

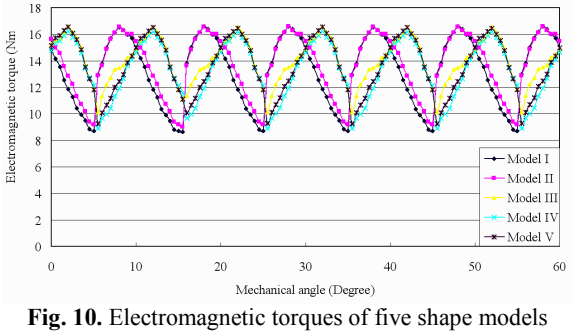

Fig. 10. Electromagnetic torques of five shape models

Conclusion

This paper has presented a novel exterior-rotor geared motor that integrates a BLPM motor with an epicyclic-type gear reducer. The geared motor possesses smaller cogging torque and

torque ripple than an existing BLPM motor that has identical magnet materials and similar motor dimensions. The proposed motor configuration helps to suppress the vibration and acoustic noise of the BLPM motor, which is of benefit to the widely applications on accurate motion and position control for geared motors. Although the presented design is an exterior-rotor geared motor, it can be extended to the integration of the interior-rotor BLPM motor with an epicyclic-type gear reducer for other applications.

Acknowledgements

The authors are grateful to the National Science Council (Taiwan, R. O. C.) for supporting this research under Grants NSC 100-2221-E-224-023 and NSC 101-2221-E-224-019.

References

[1] Jahns T. M., Soong W. L. Pulsating torque minimization techniques for permanent magnet AC motor drives – A Review. IEEE Transactions on Industrial Electronics, 43(2), 1996, p. 321-330, New York.

[2] Keyhani A., Studer C. B. Study of cogging torque in permanent magnet machines. Electric Machines and Power Systems, 27(7), 1999, p. 665-678, Washington D. C.

[3] Sakabe S., Shinoda Y., Yokoyama H. Effect of interpole on cogging torque of two-phase permanent magnet motor. Electrical Engineering in Japan, 110(4), 1990, p. 131-138, Tokyo.

[4] Rizzo M., Savini A., Turowski J. Influence of number of poles on the torque of DC brushless motors with auxiliary salient poles. IEEE Transactions on Magnetics, 27(6), 1991, p. 5420-5422, New York.

[5] Goto M., Kobayashi K. An analysis of the cogging torque of a DC motor and a new technique of reducing the cogging torque. Electrical Engineering in Japan, 103(5), 1983, p. 711-718, Tokyo.

[6] Zeroug H., Boukais B., Saharoui H. Analysis of torque ripple in a BDCM. IEEE Transactions on Magnetics, 38(2), 2002, p. 1293-1296, New York.

[7] Koh C. S., Seol J. S. New cogging-torque reduction method for brushless permanent-magnet motors. IEEE Transactions on Magnetics, 39(6), 2003, p. 3503-3506, New York.

[8] Miller T. J. E., Hendershot Jr. J. R. Design of Brushless Permanent Magnet Motors. Oxford: Clarendon Press, 1994.

[9] Hwang S. M., Eom J. B., Hwang G. B., Jeong W. B., Jung Y. H. Cogging torque and acoustic noise reduction in permanent magnet motors by teeth pairing. IEEE Transactions on Magnetics, 36(5), 2000, p. 3144-3146, New York.

[10] Li T., Slemon G. Reduction of cogging torque in permanent magnet motors. IEEE Transactions on Magnetics, 24(6), 1998, p. 2901-2903, New York.

[11] Eom J. B., Hwang S. M., Kim T. J., Jeong W. B., Kang B. S. Minimization of cogging torque in permanent magnet motors by teeth pairing and magnet arc design using genetic algorithm. Journal of Magnetism and Magnetic Materials, 226(2), 2001, p. 1229-1231, Amsterdam.

[12] Lin Y. K., Hu Y. N., Lin T. K., Lin H. N., Chang Y. H., Chen C. Y., Wang S. J., Ying T. F. A method to reduce the cogging torque of spindle motors. Journal of Magnetism and Magnetic Materials, 209(2-3), 2000, p. 180-182, Amsterdam.

[13] Hsu L. Y., Tsai M. C. Tooth shape optimization of brushless permanent magnet motors for reducing torque ripples. Journal of Magnetism and Magnetic Materials, 282(1), 2004, p. 193-197, Amsterdam.

[14] Ackermann B., Janssen J. H. H., Sottek R., Steen R. I. New technique for reduction cogging torque in a class of brushless DC motors. IEEE Proceedings – B, 339(4), 1992, p. 315-320, Stevenage.

[15] Ishikawa T., Slemon G. R. A method of reducing ripple torque in permanent magnet motors without skewing. IEEE Transactions on Magnetics, 29(2), 1993, p. 2028-2031, New York.

[16] Yan H. S., Wu Y. C. A novel configuration for a brushless DC motor with an integrated planetary gear train. Journal of Magnetism and Magnetic Materials, 301(2), 2006, p. 532-540, Amsterdam.

[17] Zhu Z. Q., Howe D. Influence of design parameters on cogging torque in permanent magnet machines. IEEE Transactions on Energy Conversion, 15(4), 2000, p. 407-412, New York.